VNIR spectral characteristics of terrestrial igneous effusive rocks: mineralogical composition and the influence of texture

C. CARLI[1]*, G. SERVENTI[2] & M. SGAVETTI[2,3]

[1]*Istituto di Astrofisica e Planetologia Spaziali-INAF Roma, Via fosso del cavaliere 100, 00133, Rome, Italy*

[2]*Dipartimento di Fisica e Scienze della Terra, Macedonio Meloni, Università degli studi di Parma, Parma, Italy*

[3]*International Research School of Planetary Sciences, Chieti-Pescara, Italy*

**Corresponding author (e-mail: cristian.carli@iaps.inaf.it)*

Abstract: Visible and Near-Infrared (VNIR) reflectance spectroscopy is an important technique with which to map mineralogy and mineralogical variations across planetary surfaces using remotely sensed data. Absorption bands in this spectral range are due to electronic or molecular processes directly related to mineral families or specific compositions. Effusive igneous rocks are widely recognized materials distributed on the surfaces of terrestrial planets, and are formed by primary minerals that can be discriminated by electronic absorptions (e.g. crystal field absorption). In this paper, we review the current knowledge of effusive rock compositions obtained by crystal field absorption in VNIR reflectance spectroscopy, and consider how different petrographical characteristics influence the mineralogical interpretation of such rock compositions. We show that: (1) the dominant mineralogy can be clearly recognized for crystalline material, especially with relatively large crystal dimension groundmass or high porphyritic index; (2) both grain and crystal size are important factors that influence the spectra of effusive rocks where groundmass is generally characterized by microscopic crystals; and (3) glassy dark components in the groundmass reduce or hide the crystal field absorption of mafic minerals or plagioclase otherwise expected to be present.

The inner solar system hosts numerous differentiated terrestrial bodies that have been shaped by widespread and often sustained volcanic activity, with a high degree of compositional variation. From Mercury to the main asteroid belt (e.g. 4Vesta), morphological and spectroscopic data provide evidence for the presence of such activity, with extrusive volcanism identified as a major process for crustal formation, consistent with the volcanic nature of the most abundantly distributed rocks. Volcanic rocks are characterized by an aphanitic texture: that is, a very fine-grained groundmass in which most of the individual crystals cannot be distinguished with the naked eye, and which is presumed to have formed by relatively fast cooling (Le Maitre *et al.* 2002). The classification of volcanic rocks is defined either by modal (QAPF diagram, indicating quartz, alkali feldspar, plagioclase and feldspathoid: Streckeisen 1978) or, more commonly, by chemical (the TAS (total alkali silica) diagram: Le Maitre *et al.* 2002) analysis. Mineral names, textural terms or other terms can also be used to distinguish further the rock type (Le Maitre *et al.* 2002). The abundance of glassy phases is also important, as is the presence of phenocrysts, which are the first crystals that form in the lava at depth, and xenocrysts, which are ripped from the crust through which lava rises.

The geological development of a planet is strongly influenced by its thermal history, which is driven by heat production, transport and loss through time. Clear phenomenological descriptions of planetary thermal histories were proposed by Sleep (2000), with those descriptions a function of primordial accretion heat loss and the radiogenic heat production budget, but also dependent on initial planetary composition and physical parameters such as lithospheric thickness (relative to planet size) and rheology. Different modes of convection related to distinct lithosphere types, including magma ocean, plate tectonics and stagnant lid, can either occur sequentially or recur cyclically throughout a planet's history, and some can be observed on different terrestrial planets today. Different forms of volcanism, as a function of different lithosphere types, are possible and are strongly related to magma composition.

Unlike other terrestrial planets, most of Earth's evolution has been, and still is, dominated by plate tectonics (e.g. Middlemost 1997). This process

From: Platz, T., Massironi, M., Byrne, P. K. & Hiesinger, H. (eds) *Volcanism and Tectonism Across the Inner Solar System*. Geological Society, London, Special Publications, **401**, http://dx.doi.org/10.1144/SP401.19

produces a broad variety of magma compositions that depend on the different conditions in which magma can differentiate, accumulate and interact with country rocks. The result is the wide compositional variation of volcanic rocks observed on Earth, from ultrabasic to acidic, and from calc-alkaline to alkaline.

However, volcanism on other bodies in the solar system is generally regarded as less diverse than that of Earth because of thermal histories that do not necessarily involve plate tectonics. For example, volcanic products on Mars are associated with basic magma compositions characterized by very long lava flows, up to around 2000 km in length (e.g. Keszthelyi *et al.* 2000). Features like lava tubes or processes such as lava flow inflation, consistent with basaltic flows, are indicative of specific emplacement mechanisms and are comparable with those recognized in terrestrial analogues (e.g. Keszthelyi 1995; Sakimoto *et al.* 1997; Sakimoto & Zuber 1998; Peitersen & Crown 1999; Giacomini *et al.* 2009).

Basic–ultrabasic compositions have been inferred for some surface units – for example Mercury's northern volcanic plains (Head *et al.* 2011; Weider *et al.* 2012) or intercrater plains – at least a portion of which is probably volcanic (Nittler *et al.* 2011; Denevi *et al.* 2013). The volcanism of these regions consists of plains with abundant flow features and buried impact craters, forming complex, kilometres-thick sets of lavas, probably emplaced in several phases (Head *et al.* 2011; Byrne *et al.* 2013). Thermal erosion (by lava, which melts, assimilates and carries away the ground rock) has been suggested as being responsible for the morphology associated with some of this volcanism, indicative of a very effusive, flood-lava-style emplacement typical of turbulent komatiitic or high-temperature mafic lavas (Groves *et al.* 1986; Head *et al.* 2011; Byrne *et al.* 2013).

The volcanic history of the Moon, like Mars and Mercury a one-plate planetary body, must be associated with melting of mantle rocks without contamination by recycled crust. The lunar surface shows a wide range of compositions generally compatible with basalt (Hiesinger & Head 2006), consistent with early Apollo observations, and the Apollo and Luna samples, which determined a basaltic nature for the maria. Lunar basaltic flows are several tens of metres thick and extend for hundreds to thousands of kilometres, with lobate fronts 10–60 m high (Schaber *et al.* 1976; Gifford & El Baz 1978). Other surficial volcanic features that may reflect a mafic origin include sinuous rilles, lava terraces, cinder cones and pyroclastic deposits (see Hiesinger & Head 2006 and references therein). Recently, Spudis *et al.* (2013) interpreted large topographical features in the lunar maria as shield volcanoes comparable to basaltic shield volcanoes on other terrestrial planets. A few domes have dimensions and structures that could be representative of more silicic lavas, of intrusion of shallow laccoliths or of large rock blocks mantled by younger lavas (e.g. Heater *et al.* 2003; Lawrence *et al.* 2005).

Compositional data from rover missions (e.g. on Mars) and laboratory sample analyses (lunar return samples or meteorite samples) provide detailed information on mineralogy, mineral chemistry and bulk-rock chemical composition, thus widening the range of recognized compositions for planetary volcanic systems. However, the analysis and mapping of surface compositions of extraterrestrial bodies in the solar system is principally based on remote-sensing surveys. Presently, the large amount of data acquired by hyperspectral sensors in the visible and near-infrared (VNIR, e.g. OMEGA spectrometer, MarsExpress; CRISM spectrometer, Mars Reconnaissance Orbiter; M^3 spectrometer, Chandrayann; VIR spectrometer, Dawn) and in the thermal infrared (TIR, e.g. TES spectrometer, Mars Global Surveyor) permit us to map these bodies at high spatial resolutions from orbit.

Most planetary bodies in the solar system have extremely tenuous or absent atmospheres and are therefore subject to space weathering at various intensities. Some effects of space weathering on the reflectance spectra of rock and regolith component minerals were experimentally analysed (e.g. Hiroi & Sasaki 2001; Sasaki *et al.* 2001; Brunetto & Strazzulla 2005; Strazzulla *et al.* 2005). For example, space weathering acts as a darkening and reddening agent of silicates, critically influencing the identification of diagnostic absorption bands in spectra of space-weathered material (e.g. Pieters *et al.* 1993; Moroz *et al.* 1996; Yamada *et al.* 1999; Pieters *et al.* 2000; Hapke 2001). Nevertheless, the variety of rock compositions in planetary crusts and regoliths raises a broader question about the intrinsic complexity of the reflectance spectra of planetary surfaces, which form the basis for investigating the spectral effects of space weathering.

In this paper, we review the compositional information that can be recognized in the VNIR spectral range for Earth's effusive basic–ultrabasic volcanic rocks. In particular, we examine to what extent absorptions indicative of the mineralogical rock-forming phases can be identified, while also considering other aspects (e.g. petrography) that can affect rock spectra in light of new data. Furthermore, we discuss both the possibilities and limits in the spectral interpretation of rocks, and present questions that are still open regarding the analysis of effusive rocks of mafic compositions. The purpose of this work is to contribute to the understanding of the

spectroscopic complexity of planetary surface compositions, and to provide a framework that can aid in the interpretation of spectra of space-weathered minerals and rocks.

The composition of effusive volcanic rocks on terrestrial bodies in the inner solar system

Initially, basalts were thought to be the primary rock type present in Martian volcanic complexes like the Tharsis province that, among other volcanic landforms, features long lava flows. Analysis of data returned by the Thermal Emission Spectrometer (TES) instrument suggested a possible compositional dichotomy between Mars' southern and northern terrains, and confirmed that the southern areas are likely to correspond to a basaltic crust, whereas the northern areas contain more evolved volcanic rocks, probably of andesitic compositions (Bandfield *et al.* 2013; Hamilton *et al.* 2001). The analysis of rocks at the Mars Pathfinder landing site also provided evidence for the presence of andesitic rocks in the Martian crust (Reider *et al.* 1997; McSween *et al.* 1999; Waenke *et al.* 2001; Foley *et al.* 2003).

Further, analysis by the Spirit rover (MER-A) of basaltic rocks in Gusev crater identified them as picritic-basalts, with evidence of olivine (ol), pyroxene (px), plagioclase (pl) and accessory oxides (McSween *et al.* 2004). Data from excavated rocks provided evidence of uniform compositions, similar to ol-phyric shergotites (McSween *et al.* 2006*a*). In addition, Spirit encountered unaltered rocks in the Columbia Hills that have been identified as members of the Wishstone, Irvine and Backstay classes (McSween *et al.* 2006*b*). These rocks are enriched in alkalis and characterized by major mineral phases including px (both low and high in Ca), sodic pl, ferroan ol and Fe–Ti–Cr oxides, as well as minor phases such as apatite, and so have been classified as tephrite, alkaline basalts and hawaiites. Some of the samples of these rocks contain glassy material (McSween *et al.* 2006*b*).

Recently, McSween *et al.* (2009) reviewed the mineral composition of Martian volcanic crust by analysing data gathered by the Spirit and Opportunity rovers, and by the gamma-ray spectrometer (GRS) on the Mars Odyssey orbiter, and concluded that the composition of the Martian crust is probably a mix of fresh and altered basaltic materials. These authors suggested that TES data could have overestimated the SiO_2 content due to superficial weathering, as no areas dominated by siliceous rocks were apparent in the GRS silica distribution map (Boynton *et al.* 2007). Mars has also been fully mapped in the VNIR at different spatial and spectral resolutions using data gathered by the OMEGA and CRISM spectrometers, and the maps of several mineral phases, including px and ol, have been published (e.g. Poulet *et al.* 2007, 2009). However, although these minerals are common on the Martian surface and constitute an important spectroscopic component of effusive rocks, there are no px or ol compositional maps available for several equatorial volcanic regions on Mars (e.g. Olympus Mons, Daedalia Planum and Elysium Mons). The presence of, at times, substantial amounts of surface dust (Ruff & Christensen 2002) and Fe^{3+} minerals (Christensen *et al.* 2000; Poulet *et al.* 2007) in these regions have both been used to explain this anomaly. Recently, in their discussion of the composition of the Daedalia Planum lava flows, Giacomini *et al.* (2012) gave evidence of px absorption bands, which suggests a variation in px composition among the different constituent lava flows. In addition, the authors demonstrated how combined spectral characteristics and morphology can be used to improve the geological mapping of the region.

The lunar crust has also been studied in detail thanks to the Apollo and Luna missions, which brought back volcanic samples containing several different rock types. Lunar rocks are generally classified into four groups. One of these groups includes a pristine volcanic basaltic rock containing both effusive and pyroclastic material (Hiesinger & Head 2006). Mare basalts are characterized by effusive textures, a high abundance of ol and px (particularly clinopyroxene (cpx)), and a relatively low content of pl as major mineral phases (Hiesinger & Head 2006). These rocks are generally enriched in FeO and TiO_2, depleted in Al_2O_3 and have high CaO/Al_2O_3 ratios with respect to other lunar compositions (Taylor *et al.* 1991 and references therein). Lunar volcanism is also characterized by pyroclastic products, which are composed of glasses with colours that vary as a function of composition and the presence of skeletal crystals (see Lucey *et al.* 2006). This volcanism is similar to terrestrial fire fountains, formed by gasses (probably CO_2 plus other minor components) contained in the rising magmas that are explosively released as they approach the surface (Nicholis & Rutherford 2005). Other volcanic products have also been identified: KREEP (potassium, rare earth elements, phosphorous) basalts enriched in incompatible elements (Warren & Wasson 1979), high potassium basalts and high-alumina basalts. KREEPs are present as small rock fragments or clasts in breccias dominated by px and pl (Shearer *et al.* 2006 and references therein). Although the origin of this material is still a matter of debate, it is thought to be the product of the melting of a hybrid lunar mantle (Shearer *et al.* 2006 and references therein).

From a geochemical point of view, mare basalts can be broadly subdivided into three groups based on TiO_2 variation (Neal & Taylor 1992): high Ti; low Ti; and very low Ti. Several papers that investigated the petrographical and mineralogical variation of the different lunar mare samples have described large variations in textures and mineralogy even within the same rock type family.

Recently, M3 hyperspectral data collected from orbit were used to map the Moon's surface, and revealed the presence of a variety of materials. In particular, mafic minerals, pl, glass and spinels were detected using crystal field (C.F.) absorption. Different maria were mapped on the basis of their different spectral signatures, which are characterized by px bands with subtle minimum shifts, and band intensity and symmetry variations. Mare Serenitas was mapped as 13 spectral units following an Integrated Band Depth analysis (Kaur *et al.* 2013). Kaur *et al.* (2013) found that mafic mineralogy varies from low- to intermediate-Ca px and, although these authors suggested that px could vary from a sub-calcic to calcic augite composition, no substantial spatial variation in composition was observed (Kaur *et al.* 2013). The band area ratio varies, indicating possible spectral variation due to the presence of ol or px with variable 1.2 μm bands.

The asteroids form a large family of distinct bodies, some of which are thought to be differentiated, which may in some cases have led to the formation of a volcanic crust. In particular, 4Vesta, recently investigated by the DAWN mission (Russell & Raymond 2011), has a heterogeneous surface. Visual and Infrared Spectrometer (VIR) data of its surface confirmed earlier Earth-based observations that linked the composition of this body with HED (howardite, eucrite and diogenite) meteorites (De Sanctis *et al.* 2012). HED meteorites are characterized by mafic achondrites with textures similar to igneous rocks. Diogenitic and cumulate eucritic samples are similar to intrusive samples. Basaltic eucrites are equivalent to effusive terrestrial rocks, whereas howardites represent brecciated samples (Mittelfehldt *et al.* 1998 and references therein). The basaltic eucrites generally show a pigeonite–pl mineralogy with textures that vary from subophitic to ophitic. Pigeonite frequently shows subsolidus exsolution of augite and an iron-rich composition. Some eucrite samples also show a relatively high ol content. Plagioclase is calcic in composition, ranging from bytownite to anorthite (Mittelfehldt *et al.* 1998 and references therein). Despite this variation in HED mineralogy, the first analyses by the DAWN mission revealed only clear px absorptions with a small minimum shift. In addition, Ammannito *et al.* (2013) recently published evidence for the presence of ol in some of Vesta's regions.

Mercury is the innermost and, until recently, the least-studied planet of the inner solar system. The importance of volcanic products on its surface was debated until remote-sensing data from the MESSENGER mission revealed the presence of extensive volcanism across its the surface (Solomon *et al.* 2008; Head *et al.* 2009; Watters *et al.* 2009). Moreover, the morphological characteristics in some regions suggested the presence of flood magmatism (Head *et al.* 2011) with possible ultramafic compositions (Nittler *et al.* 2011; Weider *et al.* 2012). However, the iron content of the rocks is still ambiguous, as reflectance and X-ray data have shown very a low FeO content (Klima *et al.* 2013; Weider *et al.* 2013), while neutron spectrometer data show substantial neutron absorption (Lawrence *et al.* 2010; Riner *et al.* 2011). Unfortunately, absorption features have not yet been identified in reflectance spectra of Mercury's surface. Therefore, the only means available with which to discriminate different lava flows and deposits are variations in surface albedo and spectral slope, which makes the task of distinguishing surface units very difficult.

On Earth, remotely sensed hyperspectral data require extensive calibration due to interference from the atmosphere, vegetation and surface water. Nevertheless, volcanic regions that have little or no vegetation have been mapped (e.g. Hawaii, Etna). Remote-sensing data, in general, show low reflectances and low spectral contrasts for mafic compositions, although different lava flows can be discriminated thanks to variations in the spectral signature of rocks with age (Abrams *et al.* 1991) and with different surface textures (Sgavetti *et al.* 2003). In addition, Sgavetti *et al.* (2003) showed that oxidation products can also be used to discriminate the distal and proximal portions of lava flows.

Spectral analyses of planetary surfaces, gathered *in situ* by rovers or in the laboratory from returned samples, have shown a wider compositional range than those predicted by remote-sensing data alone. Although indicative of a smaller range of differentiation than that of the Earth, this variation suggests a more complex volcanic history for planetary surfaces than previously thought. Focusing on VNIR spectral variations that can be linked to differences in lava compositions, textures or weathering effects permits the classification and mapping of different volcanic regions on planetary bodies.

VNIR spectroscopy of terrestrial igneous effusive rocks

The compositions of volcanic products on the different inner bodies of our solar system have

been investigated by three discrete methods: (1) remote-sensing spectroscopy; (2) *in situ* rover measurements; and (3) laboratory analysis of meteorites and lunar samples. Particular attention has been paid in such analyses to the implications of volcanism to our understanding of the evolution of planetary crusts (e.g. Mittlefehldt *et al.* 1998 and references therein; McSween *et al.* 2006*a*, *b*; Shearer *et al.* 2006 and references therein; Poulet *et al.* 2009; Kaur *et al.* 2013). The VNIR spectra of basic and ultrabasic rocks were first investigated by Hunt *et al.* (1974) using rock powder samples of different grain sizes. The spectra of intrusive rocks show well-defined features characteristic of gabbro, anorthosite and peridotite, especially for smaller grain sizes (0–74 μm), whereas effusive rocks are generally featureless with low albedo. For example, the spectral characteristics of basalts include the presence of opaque minerals and oxidation states (Hunt *et al.* 1974). In the VNIR spectra of acidic (Hunt *et al.* 1973*a*) and intermediate (Hunt *et al.* 1973*b*) igneous rocks, only a few features generally characteristic of mafic mineralogies or alteration, varying systematically across the different rock types, can be distinguished. Volcanic rocks with ultrabasic–basic compositions show a SiO_2 variation of approximately 30–52%, which can be correlated with Al_2O_3 variation, low alkali content (*c.* <5%) and a variable amount of MgO–FeO. This chemical variation reflects a mineralogy that ranges from high levels of mafic minerals (px, ol) to high levels of pl, from high magnesium to high iron, and from low to high Ca.

In this section, we summarize what has been learned about mineralogy from VNIR reflectance spectroscopy of volcanic rocks, with particular attention being paid to C.F. absorption bands of single phases, composite absorption bands due to complex mineralogies and our ability to distinguish between different absorption processes. Moreover, we discuss how textures can influence the identification of mineral phases from reflectance spectra. Further, in the following sections, 'particles' refer to synthetic mixtures of minerals prepared by weighing of individual mineral end members, where each particle represents a monomineralic sample. For rock powder samples obtained by grinding, the term 'grain' is used to refer to individual fragments, which can consist of one or more mineral ('crystal') or amorphous ('glass') phases. A grain can be mono- or multi-crystalline for wholly crystalline rocks, or mono- or multi-phase for rocks not completely crystalline. Particle or grain sizes are used to determine the granulometric range of mixtures and powder samples, respectively, whereas crystal size is used to define the size of the crystals in individual grains or in a rock slab.

Mineralogical information

In VNIR spectra, C.F. absorption bands resulting from the presence of transitional elements in well-defined coordination sites within the crystal lattice of major rock-forming minerals are recognizable (Burns 1993). In addition, other useful absorption bands indicative of compositional variation due, for example, to charge transfer (intervalence charge transfer, IVCT, between cations or between cations and ligands: see e.g. Clark 1999) can be observed in this wavelength range, as can some vibrational overtones in the OH^-, CO_3^{2-} and $S_3O_4^{2-}$ functional groups.

Volcanic rocks are generally composed of mafic silicates like px and ol, as well as some sialic minerals like feldspars, specifically calcic pl. These minerals can be characterized by C.F. absorptions due to FeO, principally, as well as TiO_2. Other transitional elements are not generally abundant enough to produce detectable absorption bands. Opaque minerals, such as Fe–Ti oxide (e.g. magnetite, ilmenite) or spinels (Cr, Mg, Al, Fe oxide), as well as Fe^{3+} or Fe^0, in the form of hematite or iron phase particles, can be present in volcanic rocks as a result of secondary processes acting in different fO_2 conditions on a planetary surface. Even if opaque minerals are generally considered neutral phases, due to their spectral characteristics and their relatively low abundances in effusive rocks, they can substantially affect albedo and spectral slope, and so mask absorption features (e.g. Cloutis & Gaffey 1991*b*). Fe^0 is a strong darkening agent and, when present in very small, nanosized particles, introduces a reddening component (e.g. Hapke 2001; Lucey & Riner 2011). Glassy phases, which are also present in both Martian and lunar samples, as well as in some meteorites, produce a darkening (general reduction of reflectance) and/or a reddening (positive spectral slope) effect in the VNIR spectra with superimposed C.F. absorption, which is thus a marker for the presence of effusive lava or pyroclastics materials (Adams & McCord 1971; Adams *et al.* 1974; Bell *et al.* 1976; McSween & Treiman 1998 and references therein; Minitti *et al.* 2002; McSween *et al.* 2004; Tompkins & Pieters 2010). This component, which is used to define textural characteristics of volcanic rocks, can also influence mineralogical information obtained from VNIR. EDQ2

Regolith that is composed of volcanic material can contain large multi-crystal or multi-phase grains that are aggregates of phenocryst fragments and submicroscopic (tens of microns) groundmass. Thus, their spectra appear similar to those acquired on cut-surfaces of rocks (i.e. slab) and are similarly affected by texture (Carli & Sgavetti 2011). In multi-crystal and multi-phase grain spectra, the

absorption features are difficult to resolve, and the continua are less predictable and poorly understood owing to the optical properties of different minerals that are aggregated. All of these phases interact with incident light, and the absorptions are the product of intimate or intraparticle mixtures. In these types of mixtures, the resulting spectra are a non-linear combination (e.g. Hapke 1993; Clark 1999). Moreover, the texture of volcanic rocks can also be characterized by iso-orientation of minerals, and the different relationships between phenocrysts, xenocrysts and the groundmass can affect the spectral signature. As a result, the spectral contrast is reduced and the known absorption structures are modified.

Detectable C.F. absorptions in ultrabasic–basic volcanic rocks

C.F. absorptions in rock-forming minerals. Rock-forming minerals (e.g. px, ol and pl) can be easily identified and used to differentiate volcanic products in the infrared portion of VNIR spectra. In addition, the spectral characteristics of these minerals and their mixtures are well known, and were reviewed in a number of papers (e.g. Crown & Pieters 1987; Cloutis & Gaffey 1991*a*, *b*; Sunshine & Pieters 1991; Burns 1993; Hiroi & Pieters 1994; Klima *et al.* 2007, 2008, 2011; Serventi *et al.* 2013*b*). All of these phases have characteristic C.F. absorptions related to the presence of Fe^{2+} in the crystal lattice (Burns 1993). In particular, mafic minerals have lower albedos and stronger absorptions than pl, which often has less than 1 wt% FeO. All of these minerals contribute to the albedo and absorption structures of rocks in the VNIR (see examples in Fig. 1).

Pyroxene is characterized by high spectral variability, which is an expression of great variability in the crystal structure, and which is, in turn, related to compositional variation. Pyroxenes can be divided into orthopyroxenes, characterized by an orthorhombic symmetry (Pbca to $P2_1/c$ structure, from high Mg to high Fe), and clinopyroxene, characterized by monoclinic symmetry (from $P2_1/c$ to $C2/c$ structure with increasing Ca) (Deer *et al.* 1992). In spectroscopy, pxs are characterized on the basis of M1 and M2 site occupancy of Fe^{2+}. Fe^{2+} prefers the M2 site in opx and in low-Ca cpx (Burns 1993), whereas it prefers the M1 site in cpx with intermediate and high Ca (and Fe) content. This behaviour means that pxs can be subdivided into two types with clearly distinct spectral signatures (Cloutis & Gaffey 1991*a*): type B, which includes phases with low–intermediate Ca content (low/intermediate Ca px) characterized by two well-defined absorptions at 1 and 2 μm; and type A, which includes high-Ca compositions (high-Ca px) characterized by a complex band at 1 μm and an absent or weak absorption at 2 μm (Cloutis & Gaffey 1991*a*; Schade *et al.* 2004). The Ca abundance is expressed by the wollastonite content (Wo%). Low-Ca px (Wo < 11%) shows the two C.F. absorption bands at approximately 0.92 and 1.90 μm, characteristic of Fe^{2+} in the M2 site. The centre of this absorption shifts from short to long wavelengths with increasing total FeO (Klima *et al.* 2007) or ferrosilite (fs%) content (Cloutis & Gaffey 1991*a*). In addition, the

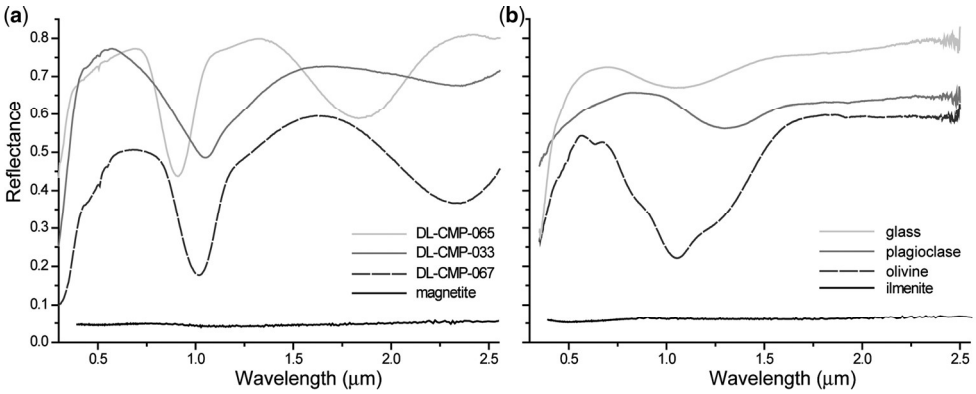

Fig. 1. Examples of mineral spectra. (**a**) pxs (opx DL-CMP-065, En_{90}; cpx DL-CMP-067, Wo_{39} En_{52} and DL-CMP-033, Wo_{49} En_{42}; particle size <40 μm) from Klima–RELAB library and magnetite from the USGS mineral library. (**b**) Anorthositic glass (FeO 1.8 wt%, g.s. particle size 20–50 μm; Carli *et al.* 2013), plagioclase (An80, FeO 0.5 wt%, 36–63 μm; Serventi *et al.* 2013*a*), olivine (Fo88, 36–63 μm; Serventi *et al.* 2013*a*) and ilmenite from the USGS library. In this box, the reflectance is shifted for clarity as follows: glass +0.1, pl +0.5 and ol −0.5.

iron content is responsible for a general decrease of albedo and the appearance of a band at about 1.2 μm (Klima *et al.* 2007).

Recently, Klima *et al.* (2011) discussed in detail the spectral variability of synthetic cpx with different Ca and Mg–Fe content. High-Ca pxs show a complex, wide and asymmetric absorption at 1 μm, and an absorption structure at approximately 1.2 μm (Klima *et al.* 2011). These authors stated that a minimum position around 1 μm could be seen for at least 2% of FeO in M2 (Klima *et al.* 2011). The band at 2 μm becomes weaker for very high wollastonite content (*c.* 50%) and is almost featureless for very high FeO content. For all cpx, increasing Fe^{2+} produces a shift in the positions of the absorption bands to longer wavelengths. An exception is high-Ca px, for which the 1 μm band position varies in a linear fashion with Wo% amount, independently of fs% (Klima *et al.* 2011).

Pyroxene C.F. absorptions were initially identified in transmittance spectra and modelled using a Gaussian distribution for each of the three different crystal orientations (Burns *et al.* 1972). Two dominant Gaussian peaks at approximately 1 and 2 μm, corresponding to Fe^{2+} absorption in the M2 site, were used for all compositions with the exception of hedembergitic compositions, which are characterized by two Gaussian peaks related to absorptions at about 0.98 and 1.2 μm, and the absence of the 2 μm absorption (Burns 1993 and references therein). In reflectance spectra, absorptions of mafic minerals have also been modelled by Gaussian distributions (e.g. MGM, Modified Gaussian Model: Sunshine *et al.* 1990; Sunshine & Pieters 1991). Two modified Gaussian peaks at 1 and 2 μm, associated with Fe^{2+} in the M2 site, plus a third Gaussian peak in the 1.2 μm region associated with absorption due to Fe^{2+} in the M1 site, are generally used (Sunshine *et al.* 1990; Klima *et al.* 2007). Klima *et al.* (2011) pointed out that for high-Ca px (e.g. augitic or diopsidic px), the 1 μm band can produce up to three different Gaussian peaks, two associated with FeO in the M1 site and one with FeO in the M2 site.

Olivine shows a wide composite absorption band in the 0.7–1.5 μm spectral range (Burns 1993) due to the presence of iron in both the M1 and M2 octahedral sites. Four different absorption positions have been identified for the different crystal orientations. For each orientation, the positions of the reflectance minima shift to longer wavelengths in a linear manner with increasing ferrous iron content (Cloutis *et al.* 1986; Burns 1993). Using an MGM-based deconvolution, Sunshine & Pieters (1998) produced a composite absorption band with three different Gaussian peaks, and reproduced the band centre shift observed by Burns (1993).

Plagioclase (pl) shows a clear absorption at around 1.25 μm, attributed to iron substituting for Ca^{2+} in the crystal lattice, that is detectable even for very low iron content (Cheek *et al.* 2011; Serventi *et al.* 2013*b*). Since pl spectra show higher albedo than those of mafic minerals, pl was generally considered a spectrally neutral phase. Moroz & Arnold (1999) discussed the effects of pl as a neutral component when mixed with an absorbing component. However, the almost 0.5 wt% FeO content of pl produces an intense absorption that can easily be recognized (Serventi *et al.* 2013*b*). Basaltic pl generally contains even higher levels of FeO (*c.* 1.0–1.5 wt%), which can substantially contribute to the reflectance spectra of effusive rocks.

Opaque minerals, particularly Fe–Ti oxide, are also present in ultrabasic and basic volcanic rocks. Oxides are generally a darkening agent in VNIR spectra, where they appear as a broad C.F. absorption band at approximately 1 μm due to FeO, and a weak absorption at about 0.6 μm due to Ti^{3+} (Burns 1993). Glass, another important component of effusive rocks, is generally characterized by an absorption structure at around 1.1 μm that is related to the presence of FeO (Bell *et al.* 1976; Dyarn & Burns 1981; Cloutis *et al.* 1990*b*; Burns 1993). In addition, glasses can also be darkening or reddening agents, as seen in the lunar glassy component (Gills-Davis *et al.* 2007, 2008; Tompkins & Pieters 2010) and in terrestrial volcanic rocks (Carli & Sgavetti 2011). The spectral variability of the glassy component is linked to composition and oxygen fugacity, although its effects on the identification of absorption structures of minerals in volcanic rocks have not been sufficiently discussed in the literature. In this paper we do not discuss hydrated mineral phases present as alteration or secondary phases seen in terrestrial rocks.

C.F. absorptions in mineral mixtures and volcanic rocks. In VNIR, volcanic rock-forming minerals absorb in a narrow spectral range in the 1 μm region (composite band) indicative of iron in M2 or M1 octahedral sites of mafic phases or in pl. There have been several studies focusing on the characterization of the spectral characteristics of mixtures between some of these compositions, by analysing mixtures of separate mineral phases of one grain size. Both the analysis of absorption band spectral parameters (reflectance, continuum slope and absorption spectral contrast) and band deconvolution by MGM (Sunshine *et al.* 1990) were used to establish possible relationships between spectral characteristics and compositions of the mineral mixtures. Distinct mixtures of two pxs (Cloutis & Gaffey 1991*b*), opx and ol (Cloutis *et al.* 1986; Moroz *et al.* 2000), pl and px (Crown &

Pieters 1987; Pompilio *et al.* 2007), and px and oxide (Cloutis *et al.* 1990*a*; Pompilio *et al.* 2007) were investigated, as well as a limited number of mixtures of three or more components (see Cloutis *et al.* 1990*b* and references therein). These papers reported semi-quantitative trends relating spectral properties to mineral compositions. It was possible to deduce these relationships because the parameters of the spectral end members are known. Trends or variations were identified for px and ol mixtures, whereas mixtures with pl were considered in only a few cases (Crown & Pieters 1987; Pompilio *et al.* 2007; Serventi *et al.* 2013*a*, *b*).

The influence of pl in mixtures with mafic minerals was investigated in detail by Serventi *et al.* (2013*a*, *b*). These authors showed the unexpected spectroscopic effects of pl chemistry superimposed over the expected effects due to mafic minerals. The greatest spectral parameter variations are seen in mixtures containing pl with high volumetric FeO concentrations, which can increase with both pl abundance and/or FeO content in pl. Moreover, these spectral variations can even be correlated to the particle size of the material.

MGM-based deconvolution of composite bands has allowed for a quantitative evaluation of the different mineral compositions in mixtures. Opx and cpx absorptions have been clearly resolved from 1.0 and 2.0 μm composite bands of these mineral mixtures by modelling the components due to Fe^{2+} in the M2 (at 1 and 2 μm) and M1 (at 1.2 μm) sites (Sunshine & Pieters 1993). In addition, a clear relationship was identified both between Gaussian peak positions and mineral compositions, and between band depths (intensity) and mineral abundances (Sunshine & Pieters 1993). Some papers have recently implemented a systematic approach using MGM for more complicated materials (e.g. Clenet *et al.* 2011), even if no papers have discussed in detailed the application of MGM to more complex composite bands due to the presence of high-Ca px, ol and pl, or more than two mineral phases.

Synthetic mixtures of minerals generally show spectral characteristics that are comparable with those of intrusive rock powders, in which crystals range in size from hundreds of microns to sizes visible to the naked eye (Fig. 2). In contrast, powder spectra of volcanic rocks show a lower reflectance and reduced spectral contrast than intrusive rock spectra for analogue grain-size ranges and similar bulk-rock compositions. In the example in Figure 3, a noritic sample and a basalt with similar SiO_2 content (see Table 1) show different bidirectional reflectance and spectral contrast but similar spectral signatures, which is in agreement with the similar amounts of pxs. The minima shifts are in agreement with the lower Ca content of noritic px.

The differences in reflectance and band intensity can be interpreted as a consequence of the increasing particle size of minerals (e.g. Craig

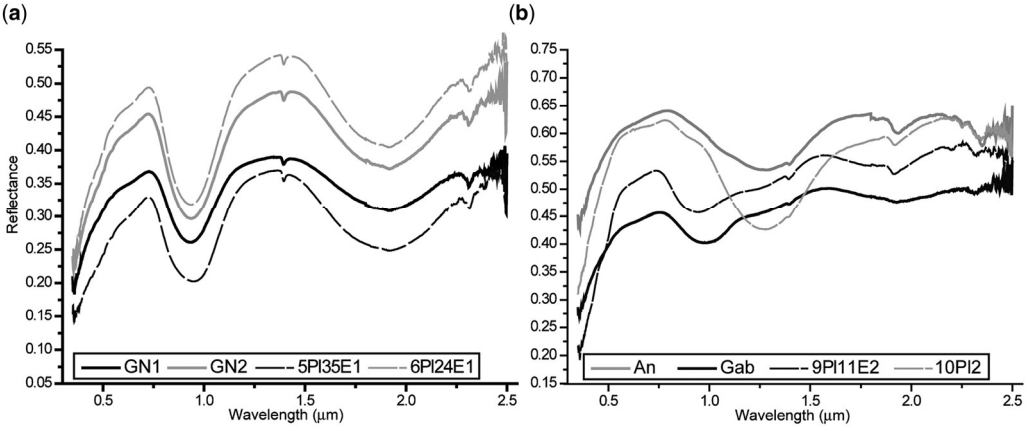

Fig. 2. An example of reflectance spectra from mineral mixtures, with particle size 250–125 μm (Serventi *et al.* 2013*b*), and rock powders, with grain size <250 μm (Carli 2009). Left box: GN1 55% pl (An80–FeO 0.36 wt%); 10% cpx ($En_{44}Wo_{46}$); 35% opx (En_{75}); GN2 61% pl (An81–FeO 0.37 wt%); 17% cpx ($En_{46}Wo_{45}$); 22% opx (En_{78}). These samples are spectrally similar (e.g. position and intensity) to mineral mixtures 5Pl35E1 and 6Pl24E1, respectively (50% Pl3, 50% E1 and 60% Pl2, 40% E1, see Serventi *et al.* 2013*b*). Right box: An (94% pl (An79–FeO 0.45 wt%), 4% cpx ($En_{42}Wo_{45}$)); Gab (81% pl (An79–FeO 0.36 wt%), 16% cpx ($En_{42}Wo_{45}$); 3% opx (En_{82})). These samples are spectrally similar (e.g. in terms of position and intensity) to mineral mixtures 10Pl2 and 9Pl11E2, respectively (100% Pl2 and 90% Pl1, 10% E2; see Serventi *et al.* 2013*b*). For clarity, the reflectance of the 6Pl24E1 and An spectra have been shifted, by +2.5% and 5%, respectively.

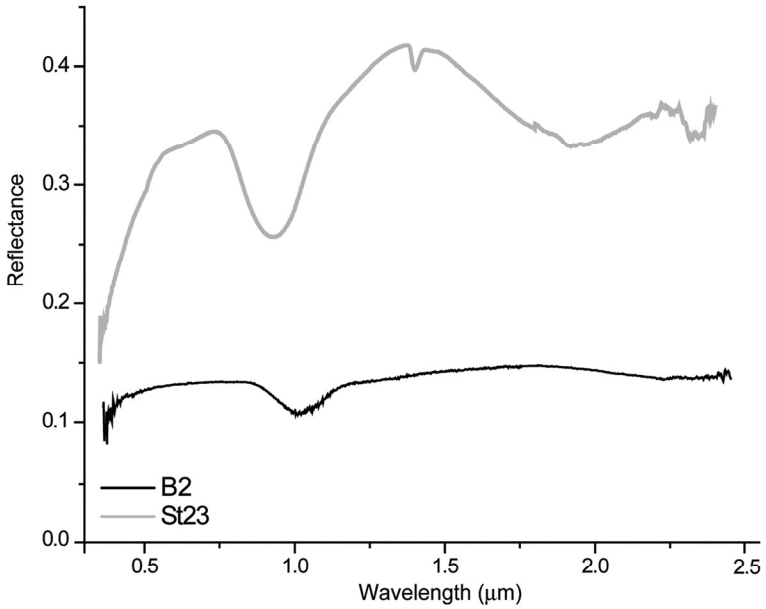

Fig. 3. An example of an intrusive cumulate mafic rock (St23 from Carli 2009) and an effusive basalt (B2; Carli & Sgavetti 2011). Both samples are characterized by px absorptions but the spectral contrast and reflectance are reduced in the effusive basalt despite similar high amount of pxs (low-Ca in St23 and intermediate-Ca in B2).

et al. 2008) and in cut-rock (slab) spectra (Sgavetti *et al.* 2006; Pompilio *et al.* 2007) rather than due to different mineralogical associations.

Spectroscopic effects of composition and petrographical parameters. In regolith, the presence of different lithologies in the same image pixel, as well as variations in grain size (from very fine powder to outcrop scale) and compositions, can influence the spectral signature in an unpredictable way. In particular, if the original rock had an aphanitic texture with a groundmass wholly characterized by crystals a few tens of microns in size, even fine-grained regoliths are spectrally controlled by multi-crystal grains that each reflect the characteristics of the rock texture (Carli & Sgavetti 2011). In such material, spectral behaviour is controlled by the effect of optical coupling (Hapke 1993 and references therein). This phenomenon is caused by the extremely close proximity of the particles, which has considerable implications for both grains and rock slabs. In this subsection we

Table 1. *XRF analysis of major elements of rocks presented in Figures 3–5*

	A2	Sal22	Et02	Et26	B2	St23	Et12	Et13	Et14	Et15
SiO_2	48.79	48.40	46.97	47.99	49.29	50.44	46.90	46.55	46.35	47.09
TiO_2	1.54	1.84	1.80	1.57	2.85	0.19	1.78	1.77	1.79	1.79
Al_2O_3	14.89	16.21	16.77	18.41	13.45	17.29	16.82	17.07	16.39	16.85
Fe_2O_{3tot}	11.95	11.86	11.69	10.30	14.82	11.24	11.47	11.35	11.62	11.51
MnO	0.19	0.16	0.19	0.17	0.22	0.14	0.19	0.19	0.19	0.19
MgO	7.53	7.66	5.35	4.59	5.60	9.75	5.63	5.26	5.82	5.64
CaO	12.75	8.95	10.20	10.18	10.19	8.76	10.40	10.03	10.45	10.47
Na_2O	2.04	3.45	3.53	3.88	2.71	1.10	3.54	3.75	3.52	3.64
K_2O	0.15	0.87	1.95	1.49	0.43	0.38	1.83	1.93	1.81	1.88
P_2O_5	0.13	0.35	0.57	0.54	0.28	0.02	0.54	0.55	0.52	0.54
Total	99.96	99.75	99.02	99.12	99.84	99.31	99.10	98.45	98.46	99.60

These measurements were made using an X-ray fluorescence spectrometer at the XRF laboratory at the Geoscience Department of the University of Padova.

discuss how it can influence a measured spectral signature.

- *Texture effects in wholly crystalline rock samples: differences between rock slab and powders.* The influence of original rock texture on the spectral features of rock powders can be clearly observed if the grain size of the powdered material is larger than the crystal size of the original rock. In this case, each grain is a multicrystal grain and will spectrally behave like the original rock. For intrusive rock, a rock slab sample larger than the illuminated spot (which must, in turn, be larger than the individual crystals) will have a spectrum affected by the spectroscopic interaction of electromagnetic energy with the rock component minerals (i.e. single crystals) along the optical path of the light. This generally results in a blue slope, and substantially reduced reflectance and spectral contrast, which further decrease at longer wavelengths resulting in the suppression of some diagnostic absorptions (Yon & Pieters 1988; Pompilio *et al.* 2007). In contrast, the same rock powder sample with grain size close to or smaller than the crystal size will behave similarly to an intimate mixture of single mineral particles, producing a spectrum in which the spectral bands of the distinct phases can be recognized.

  The change in slope between slab and powder rock sample spectra, although well documented by Harloff & Arnold (2001) and Pompilio *et al.* (2007) for both effusive and intrusive rocks, is still unexplained. Increasing opaque mineral concentrations, variation in iron-bearing silicate abundances and alteration due to weathering of some minerals (e.g. serpentinization) have been proposed as possible causes of the reduction in compositional information to the point of producing featureless spectra for intrusive slab samples (Carli & Sgavetti 2011). Moreover, rocks with very different compositions can converge to very similar spectral features, whereas powders of the same rocks can display clearly distinct spectral characteristics. Pompilio *et al.* (2007) also stated that absorption minima in slab spectra shift to slightly higher wavelengths with respect to those of powder spectra, relating this shift to the strongly negative slope observed in slab spectra. Carli *et al.* (2012) clearly showed that it is possible to distinguish the 1 μm absorption bands due to px in both powder and slab spectra of different rocks belonging to the gabbro–norite series by applying Gaussian models (e.g. MGM). The absorption positions are also comparable with those measured for pure minerals, apart for slight differences in positions between powders and slabs (Cloutis & Gaffey 1991*a*). In addition, the intensity of the absorption band in slab samples is reduced, whereas attenuation increases with the iron content.
- *Texture effects in wholly crystalline rock samples: effects related to grain size and roughness.* Regolith crystal and grain size can play a crucial role in the interpretation of absorption features in the spectra of effusive rock samples. However, Figure 4 shows that effusive rocks with different crystal sizes, but with holocrystalline texture and similar bulk-rock compositions, can have different spectral characteristics. The spectra in Figure 4 were acquired from slab samples at S.Lab. (Spectroscopy Laboratory, at IAPS–INAF in Rome), using a Fieldspec Pro mounted on a goniometer, with incidence angle (i) = 30°, emission angle (e) = 0° and an illuminated spot of approximately 0.5 cm^2, at standard conditions. The samples were illuminated with a QTH (quartz tungsten halogen) lamp (see Carli & Sgavetti 2011 for more details on sample preparation and laboratory set-up).

  The grain-size effect in single mineral phases is well studied (e.g. Craig *et al.* 2008), whereas only a few papers have addressed the effects of grain size in rock powders and roughness variation in slabs. Harloff & Arnold (2001) measured the specular reflectance for both different pxs and for basalts, and related the reflectance, the continuum and the band depth to the powder grain size and to slab roughness in all the samples. These authors also showed that reflectance increases with decreasing grain size and roughness, whereas the continuum and the band depth increase with increasing grain size and roughness up to a maximum before dropping off. Carli & Sgavetti (2011) discussed spectral characteristics measured in bidirectional reflectance with $i = 30°$ and $e = 0°$ for basaltic samples with similar textures and different compositions, as well as for basaltic samples with different textures and similar compositions. For all samples, the slab spectra showed the lowest reflectance, although samples with larger grain sizes (<2.00 mm) displayed spectral characteristics (including reflectance, slope and band intensity) very similar to those of the slab spectra. These results suggest that rock-related optical coupling (Hapke 1993) must be taken into account even for regolith with grain sizes on the order of millimetres.

  It is therefore evident that, for effusive rock powders with a grain size that is comparable to crystal size, the spectral signature is controlled by mineralogy and characterized by a reflectance that varies as a function of particle size. However, if the crystal size is smaller than the

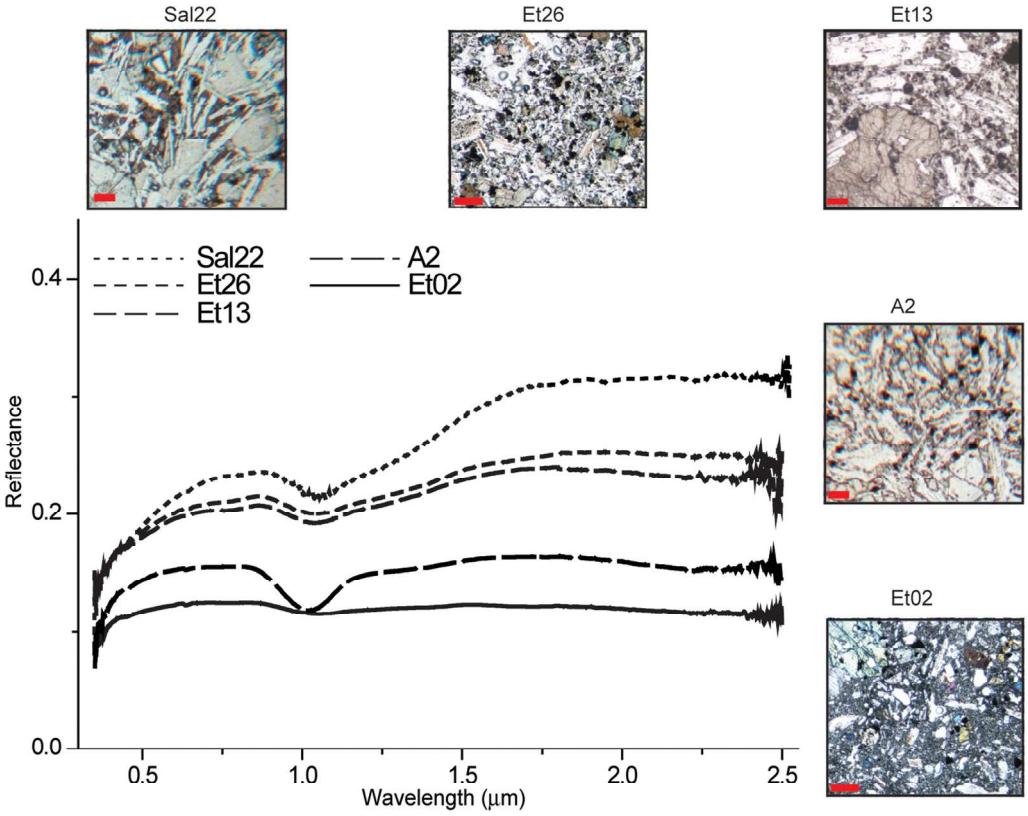

Colour online/ colour hardcopy

Fig. 4. Volcanic rocks with very similar bulk-rock compositions (see Table 1) but different crystal sizes and/or P.I. and/or relative mineral abundances. In the thin-section images, spectral variation depends not only on composition but also on the different volcanic conditions that generate mineral and texture variations. The A2 and Sal22 samples are from Iceland and Payun Matru (Argentina), respectively (see fig. 1 in Carli & Sgavetti 2011). The Et02 sample is from Etna's 2002 lava flow, Et26 is from Etna's 1665 lava flow and Et13 is from Etna's 1983 lava flow. In all thin section images, the red scale bar denotes 200 μm.

maximum grain size, a large number of mixed grains are expected to be present, resulting in spectral information that is strongly affected by optical coupling.

- *Texture effects in wholly crystalline rock samples: influence of pheno- and xenocryst*. Another important factor to consider when interpreting the spectra of effusive rocks is the relationship between groundmass, phenocrysts and xenocrysts. Phenocrysts are minerals that crystalize in equilibrium with magma, generally in the deep crust. Xenocrysts, however, are minerals that have been dislodged from the walls of the magma conduit during magma ascent. The % abundance of phenocrysts with respect to the groundmass defines the porphyritic index (P.I.) of a lava, an important parameter that indicates the degree of crystallization of the rising magma.

From a spectral point of view, lavas with a porphyritic texture (high P.I.) are expected to have a reflectance and a spectral contrast that are very close to those of intrusive rocks. Unfortunately, no studies addressing this topic in detail have yet been published. Carli & Sgavetti (2011) pointed out that fine-grained rock samples with a small percentage of millimetre-size phenocrysts have spectral signatures dominated by absorptions characteristic of the mineral phases composing the phenocrysts. In contrast, spectra of the same rocks taken from coarse-grained powder samples are dominated by the groundmass. This is probably due to a pre-eminence of multi-crystal grains in coarser-grained samples, which produce a strong signal that greatly subdues or completely masks the phenocryst signature.

- *Texture effects in partly amorphous rock samples: how groundmass, glassy component and crystal size work*. The groundmass composition and crystallinity of volcanic rocks can strongly

affect the mineralogical information that we can retrieve from reflectance spectra. The groundmass is the fine-grained matrix within which larger crystals are embedded. Mineral crystal size can vary from a few microns to tens of microns or larger. Glassy material can also be an important component because it defines the groundmass texture, which can be holocrystalline, hypocrystalline, vitrophyric or holohyaline (in order of increasing glass content). Moreover, this component is frequently characterized by oxide microphases (tachylitic glass), which are unresolvable even under high-magnification optical microscopy. Both the glassy component and the fine-grained groundmass contribute to a general darkening of the effusive samples and a lowering in the intensity of C.F. absorptions, at times resulting in featureless spectra, which complicates the spectroscopic analysis of these rocks. However, Carli & Sgavetti (2011) pointed out that two basaltic samples with similar compositions but different groundmass textures have different spectral characteristics in the VNIR.

Here, we discuss in detail some effects of rock texture in four different samples belonging to a Mt Etna lava flow from the 1983 event. The spectra of rock powder samples (<0.250 mm) are shown in Figure 5. Powders were prepared by grinding and sieving representative rock portions in a 0.250 mm sieve. The spectra were acquired with the same experimental set-up as that described for Figure 4 (see Carli & Sgavetti 2011 for more details on sample preparation and laboratory set-up). The original rock samples were collected at different locations along a vertical section going from the inner to the outer part of a 1.5 m-thick lava flow. The four samples (Et13, Et14, Et12 and Et15 from in to outside) show similar mineral assemblages: pl, cpx, minor ol and oxides. The groundmass varies from holocrystalline to hyalopilitic and vitrophyric, with a tachylitic glass.

The bulk-rock compositions reported in Table 1 show homogeneous major-element chemistry. Table 2 and Figure 6 give the compositions of the major mineral phases, and show overlapping mineral chemistries of all the samples, with small variations between phenocrysts and microcrystals. Clinopyroxene is a diopsidic augite with very little variation in the Wo_{44-46} and En_{37-40} components, whereas pl has a compositional range that varies from An50 to An80, with average FeO close to 0.7 wt% for all the samples. Olivine compositions are also very similar: Fo70 for all of the samples except Et12, which is slightly richer in Mg (Fo77). SEM images of thin sections were collected to determine the P.I. and to qualitatively describe the

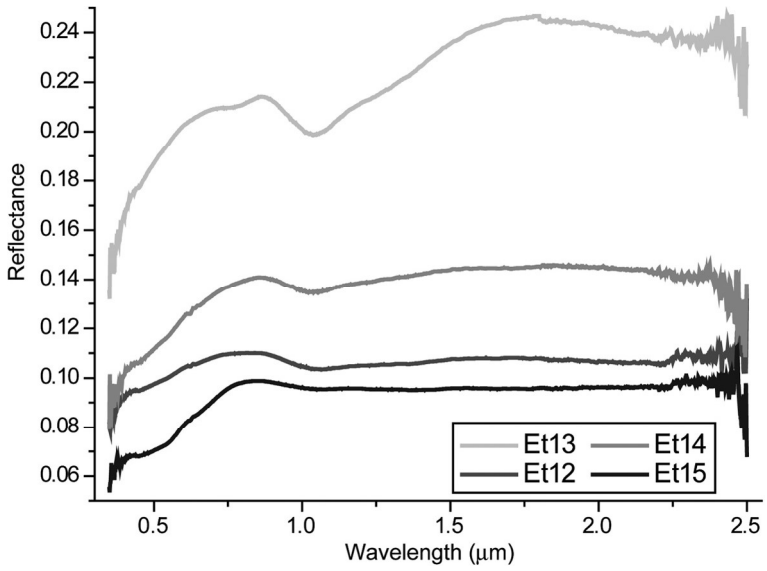

Fig. 5. Spectra of four different samples from a Mount Etna lava flow. The samples have very similar P.I., with similar relative mineral associations, but with different groundmass textures. The intensity of the C.F. composite band, which is due to mafic and pl mineralogy, is strongly reduced from sample Et13 to Et15, increasing the tachylitic glass content in the groundmass of these samples (see also Fig. 6 and Tables 2 & 3). These spectra were acquired with a FieldspecPro® $i = 30^{\circ}$, $e = 0^{\circ}$, white Spectralon standard Labsphere®, QTH lamp, at SLAB, IAPS–INAF, Rome.

Table 2. *Average composition for the major mineral phases present as pheno- and microcrysts*

	Clinopyroxene					Olivine					Plagioclase			
	Et12	Et13	Et14	Et15		Et12	Et13	Et14	Et15		Et12	Et13	Et14	Et15
SiO_2	48.21	48.60	46.98	48.34		38.72	37.35	37.60	37.94		51.92	51.57	50.58	50.93
TiO_2	1.60	1.65	2.07	1.63		0.05	0.03	0.04	0.03		0.10	0.09	0.08	0.10
Al_2O_3	4.53	4.70	4.81	5.36		0.03	0.31	0.02	0.02		28.79	29.76	30.58	29.67
Cr_2O_3	0.02	0.02	0.01	0.01		0.00	0.01	0.01	0.02		0.01	0.02	0.01	0.01
FeO_{tot}	8.57	8.66	9.97	8.05		20.42	27.71	26.12	25.33		0.70	0.68	0.62	0.70
Mno	0.19	0.21	0.21	0.23		0.32	0.67	0.60	0.60		0.02	0.01	0.01	0.01
MgO	13.26	13.15	12.94	13.63		40.56	33.78	36.14	37.37		0.08	0.07	0.07	0.09
CaO	21.73	21.46	20.88	21.84		0.26	0.49	0.35	0.35		11.92	12.45	13.29	13.11
Na_2O	0.59	0.63	0.63	0.59		0.01	0.06	0.02	0.02		4.24	4.06	3.67	3.73
K_2O	0.05	0.03	0.03	0.02							0.61	0.37	0.29	0.37
Total	99.40	99.44	99.08	100.15		100.37	100.42	100.91	101.69		98.39	99.09	99.19	98.71
Wo	46.37	46.15	44.76	46.41						Ab	37.73	36.25	32.73	33.21
En	39.34	39.29	38.60	40.23	Fo	77.95	68.14	71.09	72.45	An	58.67	61.56	65.56	64.61
Fs	14.29	14.56	16.64	13.36	Fa	22.05	31.86	28.91	27.55	Or	3.60	2.19	1.71	2.18

The mineral chemistry was determined by electron microprobe analyses with a CAMECA SX50 (EMP) at the microprobe laboratory of CNR–IGG, Padova.

groundmass characteristics over a representative area of each sample. Phenocryst abundances were calculated from compositional maps collected for major elements (Si, Al, Ca, Na, Mg, Fe and Ti). Red–green–blue (RGB) images and single-channel images were generated using the ENVI® software, and phenocrysts with different mineral chemistries were distinguished from the sample's cavity by processing the images with ImageJ®. The areal abundances of each phase were calculated and are reported in Table 3. The P.I. varies from 36 to 41%. Moreover, pl abundances are 21–27%, whereas those of mafic minerals, composed almost entirely of cpx (*c.* 90%), have abundances of

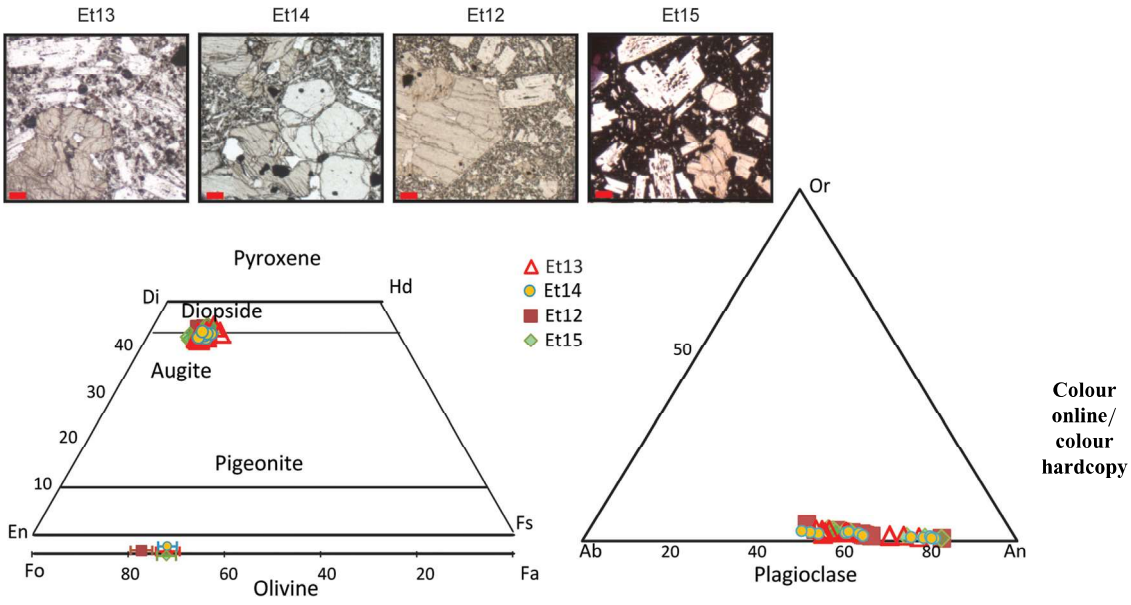

Colour online/ colour hardcopy

Fig. 6. The px, ol and pl composition of Etna samples (see also Table 3). Thin-section images show the groundmass texture variation from holocrystaline (Et13) to vitrophyric (Et15). As before, the red scale bar in the thin section images denotes 200 μm.

Table 3. *Areal abundances of phenocrysts present on Etna samples and holes*

	Pl (%)	Cpx + ol (%)	Ox (%)	Hole (%)	Σ (PhX%)
PhX _Et13	26.91	11.26	1.12		39.28
PhX _Et14	22.10	12.35	0.90	1.50	35.35
PhX _Et12	21.00	13.46	1.83	5.10	36.28
PhX _Et15	24.47	16.11	0.81	8.07	41.39

Holes indicate sample cavity. The rest is the groundmass, which varies from all microcrystalline to very high glass component from Et13 to Et15. A threshold of 20 pixels was used as a minimum area to be considered.

11–16%. All of the samples show a very similar phenocryst abundance that is consistent with the spectral variation observed, which is mainly controlled by differences in the groundmasses.

In the sample spectra (Fig. 5), despite identical mineralogical and bulk compositions and similar phenocryst distributions, reflectance varies from approximately 22 to 9% at 0.8 μm. In sample Et13, the wide absorption centred at 1.037 μm is consistent with the presence of cpx and ol. Samples Et14 and Et12 also show a minimum in a similar position, but the spectral contrast between the shoulders and the minimum is greatly reduced. Finally, Et15 shows a very weak, almost featureless, band at wavelengths longer than 0.80 μm, with a minimum at 1.05 μm. The 1 μm Band Area was calculated as the integrated area delimited by a linear continuum between the band onset and offset. The Band Area varies from 4% for sample Et13, to 2% for Et14 and Et12, and 1% for Et15, indicating a clear reduction of spectral information due to the glassy component of the groundmass.

Discussion

Several papers have been published that focus on spectral reflectance characteristics of rock-forming minerals (e.g. px, ol and pl) from effusive rocks, with some also discussing the spectral characteristics of these bulk rocks. Several points must still be clarified, however, to allow for a better interpretation of the information contained in remote-sensing data. On Mars, ol or px spectroscopic indexes of regions with volcanic edifices have not been mapped despite well-established evidence for the presence of basalts on the planet. In contrast, the spectra of lunar maria and the surface of Vesta clearly show the presence of px absorptions but not the presence of ol, although ol eucrite and ol lunar basalts are well documented by rock sample and meteorite analyses. However, compositional interpretation has been generally based on spectroscopic criteria that do not take into consideration the specific petrographical characteristics of volcanic rocks. Basic–ultrabasic volcanic rocks are, in fact, characterized by relatively high levels of mafic minerals with variable amounts of pl, which increase from ultrabasic to basic compositions. However, texture can influence spectra by modifying the spectral slope and reducing or extinguishing band intensities, which facilitates the recognition of some mineral phases over others.

Spectral reflectance studies of Earth's basic–ultrabasic rocks have contributed to a substantial improvement in the understanding of this topic. Spectral knowledge of these rocks to date, from literature and this study, can be summarized as follows:

- For volcanic rocks with holocrystalline texture:
  - the presence of the 1 and 2 μm bands is indicative of the occurrence of px, whereas a wide composite band at 1 μm indicates the presence of ol. The absence of the 2 μm band in a spectrum can be interpreted as the result of the presence of high-Ca px ± ol (e.g. Hunt *et al.* 1974; Harloff & Arnold 2001; Carli & Sgavetti 2011). Similar bulk-rock chemical compositions have spectra with different absorption features (e.g. Figs 4 & 5) because different magma chamber depths, crystal fractionation and cooling histories lead to different mineral abundances and/or chemistries (i.e. the presence of px with different composition and/or ol, as ground mass and/or phenocrysts);
  - the spectra of powders of effusive rocks with groundmass crystal sizes of hundreds of microns are similar to those of intrusive rock powders, and are also similar to those of synthetic mixtures of minerals (i.e. to gabbro or to gabbronorite ± ol) (see the subsection on 'C.F. absorptions in mineral mixtures and volcanic rocks'). If the crystals in the groundmass are tens of microns in size, even the fine-grained powders will contain multi-crystal grains. This results in a reduction in albedo and in spectral contrast, although the predominant mafic mineralogy can still be resolved (e.g. see Et13 in Fig. 5: see also Carli & Sgavetti 2011);

  - the P.I. can also play an important role: with increasing P.I., phenocryst absorptions become more apparent, and mafic minerals with abundances of just a few per cent dominate the spectra of intermediate- to fine-grained powders (see the subsection on 'Spectroscopic effects of composition and petrographical parameters': see also Carli & Sgavetti 2011). In contrast, when the powder grain size is considerably larger than the crystal size, optical coupling strongly influences the spectral signature and so the groundmass dominates the spectral characteristics (see 'Spectroscopic effects of composition and petrographic parameters').
- The presence of glass (i.e. tachylite) in a groundmass substantially modifies its petrographical texture and strongly affects the spectral information, as reported by Carli & Sgavetti (2011) and discussed in detail in the subsection on 'Spectroscopic effects of composition and petrographical parameters'. The sample set discussed there comes from the same lava flow, and is thus characterized by very similar P.I., mineralogical associations and identical bulk-rock chemical compositions. Nevertheless, with increasing glass contents in the sample groundmass, from low (e.g. Et14: hyalopilitic groundmass) to high (e.g. Et15: vitrophyric groundmass) glass, the spectral shape is modified from a low-reflectance spectrum with a strongly reduced 1 μm band to a darker, almost featureless spectrum.

As mentioned above, remotely acquired spectral reflectance data are often analysed using specific indexes to identify diagnostic absorptions. However, these indexes can be difficult to apply when several compositional and petrographical factors in outcropping rocks and in regolith interplay, resulting in a reduction of the mineralogical information contained in the VNIR reflectance spectra. In order to characterize the composition of an area, VNIR reflectance spectroscopy should be used in concert with geomorphological studies to identify end-member geomorphic units over which spectral units containing the mineralogical information can be draped, so as to substantially increase the geological significance of the resulting geomorphic–spectral units (e.g. Giacomini *et al.* 2012). Future missions will carry hyperspectral sensors for *in situ* rock analyses (e.g. the Ma_MISS (Corradini *et al.* 2011) and MicrOmega (Pilorget *et al.* 2012) instruments on the ExoMars 2018 rover). Any spectroscopic data acquired by future rover missions will be strongly affected by the rock petrographical characteristic of the surface rocks, particularly by volcanic rocks. Since these rocks are expected to be the most abundant materials on terrestrial planets, more studies aimed at exploring the effects of texture on mineralogy at different spatial resolutions are needed in order to better interpret spectral data collected both from orbit and by rovers. As a final consideration, improvements in the spectroscopic characterization of volcanic rocks, by taking into consideration different chemical compositions and different mineral assemblages, will help further inform the analysis and identification of effusive lithologies using both direct (e.g. specific absorption bands) and indirect (e.g. typical reflectance, spectral slope and mineral alterations) information.

Implications

The surfaces of inner solar system bodies are extensively covered by volcanic products with variable compositions and petrographical characteristics that can be analysed using high-resolution spectroscopic data. VNIR absorptions permit the identification of some of the spectroscopically dominant minerals in the rocks. This allows us to discriminate px-rich (pigeonitic or augitic) and ol-rich volcanic rock compositions within basic–ultrabasic effusive materials with holocrystalline groundmasses. The relationship between the 1 and 2 μm bands can also be helpful, by signalling the presence or absence of low- to intermediate-Ca px. Reflectance and spectral contrast can be directly related to the P.I. and the crystal size of the groundmass. For samples with a very fine groundmass and with tachylitic glass, the spectral absorptions are reduced to a featureless spectrum, masking the expected absorptions of the mineral phases.

Because of the improved spatial resolution of remote-sensing data, and the use of hyperspectral sensors on rovers to investigate volcanic rocks in greater detail, further work should be focused on finding both direct and indirect evidence of compositional evolution of magmatic processes. To accomplish this, as well as to better explore planetary volcanic regions using VNIR spectroscopy and to discriminate among the effusive products, major effort should be made to:

- understand the 'abundance limits' for mafic mineralogies (by separating e.g. ol-poor from ol-rich rocks, alkaline from subalkaline rocks, and iron-poor from iron-rich magmatism);
- understand the limit (e.g. the chemistry and relative abundance) beyond which pheno- or xenocrystal compositions have a greater effect on the spectral signature than groundmass mineralogy – for example, future work should investigate how the spectral signature varies between massive basalts with similar compositions and

mineralogical assemblages, but different P.I., in order to understand how spectral information is influenced by different crystal distribution in the rock; and

- investigate the relationship between crystal size and grain size in particulate soils (like regoliths) derived from effusive igneous rocks in order to determine the most suitable conditions for obtaining diagnostic spectral information that would be more reliable than information provided by synthetic mixtures of minerals, which are more comparable with intrusive igneous rocks.

These efforts could produce a standard of information for volcanic compositions from which to begin the investigation of weathering effects on the spectra of effusive igneous rocks. We suggest that integrating and comparing geomorphic volcanic units and spectral units of compositional significance is the most reliable approach for geological mapping of volcanic regions on planetary surfaces, as already demonstrated by Giacomini *et al.* (2012).

The authors would like to thank L. Peruzzo for a useful introduction to the use of the SEM at the GeoScience Department of the University of Padua. Financial support was perovided by Agenzia Spaziale Italiana, SIMBIO-SYS project. The authors would also like to thank two anonymous reviewers, and P. K. Byrne and T. Platz, for their helpful suggestions that improved this manuscript.

References

Abrams, M., Abbott, E. & Kahle, A. 1991. Combined use of visible, reflected infrared, and thermal infrared images for mapping Hawaiian lava flows. *Journal of Geophysical Research*, **96**, 475–484.

Adams, J. B. & McCord, T. B. 1971. Optical properties of mineral separates, glass, and anorthositic fragments from Apollo mare samples. *In*: *Proceedings of the 2nd Lunar Science Conference*, *Volume 3*. MIT Press, Cambridge, MA, 2183–2195.

Adams, J. B., Pieters, C. M. & McCord, T. B. 1974. Orange Glass: evidence for regional deposits of pyroclastic origin on the Moon. *In*: *Proceedings of the 5th Lunar Science Conference, Houston, Texas, March 18–22, 1974, Volume 1*. Pergamon Press, New York, 177–186.

Ammannito, E., De Sanctis, M. C. *et al.* 2013. Olivine in an unexpected location on Vesta's surface. *Nature*, **504**, 122–125, http://dx.doi.org/10.1038/nature12665

Bandfield, J. L., Hamilton, V. E. & Christensen, P. R. 2013. A global view of Martian surface compositions from MGS-TES. *Science*, **287**, 1626–1630.

Bell, P. M., Mao, H. K. & Weeks, R. A. 1976. Optical spectra and electron paramagnetic resonance of lunar and synthetic glasses: a study of the effects of controlled atmosphere, composition, and temperature. *In*: *Proceedings of the 7th Lunar Science Conference, Houston, Texas, March 15–19, 1976, Volume 3*. Pergamon Press, New York, 2543–2559.

Boynton, W. V., Taylor, G. J. *et al.* 2007. Concentration of H, Si, Cl, K, Fe, and Th in the low- and mid-latitude regions of Mars. *Journal of Geophysical Research*, **112**, E12S99, http://dx.doi.org/10.1029/2007JE002887

Brunetto, R. & Strazzulla, G. 2005. Elastic collisions in ion irradiation experiments: a mechanism for space weathering of silicates. *Icarus*, **179**, 265–273.

Burns, R. G. 1993. *Mineralogical Applications of Crystal Field Theory*. Cambridge University Press, Cambridge.

Burns, R. G., Abu-Edi, R. M. & Huggins, F. E. 1972. Crystal field spectra of lunar pyroxenes. *In*: *Proceedings of the 3rd Lunar Science Conference, Volume 1*. MIT Press, Cambridge, MA, 533–543.

Byrne, P. K., Klimczak, C. *et al.* 2013. An Assemblage of lava flow features on Mercury. *Journal of Geophysical Research*, **118**, 1303–1322, http://dx.doi.org/10.1002/jgre.20052

Carli, C. 2009. *Analisi spettroscopica nel VNIR di rocce ignee: Caratterizzazione composizionale della superficie dei pianeti terrestri*. PhD thesis, University of Parma.

Carli, C. & Sgavetti, M. 2011. Spectral characteristics of rocks: effects of composition and texture and implications for the interpretation of planet surface compositions. *Icarus*, **211**, 1034–1048.

Carli, C., Sgavetti, M., Capaccioni, F. & Serventi, G. 2012. Studying Spectral Variability of an Igneous Stratified Complex as a Tool to Maps Lunar Highlands. Abstract 9007, presented at the Second Conference on the Lunar Highland Crust, Bozeman, Montana, July 13–15, 2012.

Carli, C., Roush, T. & Capaccioni, F. 2013. Retrieving Optical Constants of Glasses with Variable Iron Abundance. Abstract 1918, presented at the 44th Conference on Lunar Planetary Science, Woodlands, Texas. March 18–22, 2013.

Cheek, L. C., Pieters, C. M., Parman, S. W., Dyar, M. D., Speicher, E. A. & Cooper, R. F. 2011. Spectral Characteristics of Pl with Variable Iron Content: Application to the Remote Sensing of the Lunar Crust. Abstract 1617, presented at the 42nd Conference on Lunar Planetary Science, Woodlands, Texas, March 7–11, 2011.

Christensen, P. R., Bandfield, J. L. *et al.* 2000. Detection of crystalline hematite mineralization on Mars by the Thermal Emission Spectrometer: evidence for near-surface water. *Journal of Geophysical Research*, **105**, 9623–9642.

Clark, R. N. 1999. Chapter 1: Spectroscopy of rocks and minerals, and principles of spectroscopy. *In*: Rencz, A. Z. (ed.) *Manual of Remote Sensing, Volume 3, Remote Sensing for the Earth Sciences*. Wiley, New York, 3–58.

Clenet, H., Pinet, P., Dydou, Y., Heuripeau, F., Rosemberg, C., Baratoux, D. & Chevrel, S. 2011. A new systematic approach using the Modified Gaussian Model: insight for the characterization of chemical composition of olivines, pyroxenes and olivine–

pyroxene mixtures. *Icarus*, **213**, 404–422, http://dx.doi.org/10.1016/j.icarus.2011.03.002

Cloutis, E. A. & Gaffey, M. J. 1991*a*. Pyroxene spectroscopy revisited: spectral-compositional combinations and relationships to geothermometry. *Journal of Geophysical Research*, **96**, 22 809–22 826.

Cloutis, E. A. & Gaffey, M. J. 1991*b*. Spectral compositional variations in the constituent minerals of mafic and ultramafic assembleages and remote sensing implications. *Earth, Moon, and Planets*, **53**, 11–53.

Cloutis, E. A., Gaffey, M. J., Jackowski, T. L. & Reed, K. L. 1986. Calibrations of phase abundance, composition, and particle size distribution of Olivine-Orthopyroxene mixtures from reflectance spectra. *Journal of Geophysical Research*, **91**, 11 641–11 653.

Cloutis, E. A., Gaffey, M. J., Smith, D. G. W. & Lambert, R. S. J. 1990*a*. Reflectance spectra of mafic silicate-opaque assemblages with applications to meteorite spectra. *Icarus*, **84**, 315–333.

Cloutis, E. A., Gaffey, M. J., Smith, D. G. W. & Lambert, R. S. J. 1990*b*. Reflectance spectra of gass-bearing mafic silicate mixtures and spectral deconvolution procedures. *Icarus*, **86**, 383–401.

Corradini, A., Ammannito, E. *et al.* 2011. Ma_Miss Experiment: Miniaturized Imaging Spectrometer for Subsurface Studies. Abstract 1125, presented at the EPSC–DPS 6 Joint Meeting, Nantes, France, 2–7 October 2011.

Craig, M. A., Cloutis, E. A., Reddy, V., Bailey, D. T. & Gaffey, M. J. 2008. The Effects of Grain Size, <10 μm–4.75 mm, on the Reflectance Spectrum of Planetary Analogs from 0.35–2.5 μm. Abstract 1356, presented at the 38th Conference on Lunar Planetary Science, League City, Texas, March 12–16, 2007.

Crown, D. A. & Pieters, C. M. 1987. Spectral properties of PL and pyroxene mixtures and the interpretation of lunar soil spectra. *Icarus*, **72**, 492–506.

De Sanctis, M. C., Ammannito, E. *et al.* 2012. Spectroscopic characterization of mineralogy and its diversity across Vesta. *Science*, **336**, 697–700, http://dx.doi.org/10.1126/science.1219270

Deer, W. A., Howie, R. A. & Zussman, J. 1992. *An Introduction to the Rock-Forming Minerals*. Longman, Harlow.

Denevi, B. W., Ernst, C. M. *et al.* 2013. The distribution and origin of smooth plains on Mercury. *Journal of Geophysical Research*, **118**, 891–907, http://dx.doi.org/10.1002/jgre.20075

Dyar, M. D. & Burns, R. G. 1981. Coordination chemistry of iron in glasses contributing to remote sensed spectra of the moon. *In*: *Proceedings of the 12th Lunar Science Conference, Houston, Texas, March 16–20, 1981*. Pergamon Press, New York, 695–702.

Foley, C. N., Economou, T. & Clayton, R. N. 2003. Final chemical results from the Mars Pathfinder alpha proton X-ray spectrometer. *Journal of Geophysical Research*, **108**, 8096.

Giacomini, L., Massironi, M., Martellato, E., Pasquarè, G., Frigeri, A. & Cremonese, G. 2009. Inflated flows on Daedalia Planum (Mars)? Clues from a comparative analysis with the payen volcanic complex (Argentina). *Planetary Space Science*, **57**, 556–570.

Giacomini, L., Carli, C., Massironi, M. & Sgavetti, M. 2012. Spectral analysis and geological mapping of the Daedalia Planum lava field (Mars) using OMEGA data. *Icarus*, **220**, 679–693, http://dx.doi.org/10.1016/j.icarus.2012.06.010

Gifford, A. W. & El-Baz, F. 1978. Thickness of mare flow fronts. In: *Proceedings of the 9th Lunar Planetary Science Conference, Houston, Texas, March 13–17, 1978*. Lunar and Planetary Institute, Houston, TX, 382–384.

Gillis-Davis, J. J., Lucey, P. G., Hammer, J. E. & Wilcox, B. B. 2007. Syntheses and Reflectance Analyses of Lunar Red Glass Compositions: Information to Improve Understanding of Remotely Sensed Spectral Data. Abstract 1443, presented at the 38th Conference on Lunar Planetary Science, League City, Texas, March 12–16, 2007.

Gillis-Davis, J. J., Lucey, P. G., Hammer, J. E. & Denevi, B. B. 2008. Syntheses and Reflectance Analyses of Lunar Green Glass Compositions: Information to Improve Understanding of Remotely Sensed Spectral Data. Abstract 1535, presented at the 39th Conference on Lunar Planetary Science, League City, Texas, March 10–14, 2008.

Groves, D. I., Korkiakoski, E. A., McNaughton, N. J., Lesher, C. M. & Cowden, A. 1986. Thermal erosion by komatiites at Kambalda, Western Australia and the genesis of nickel ores. *Nature*, **319**, 136–137.

Hamilton, V. E., Wyatt, M. B., McSween, H. Y., Jr. & Christensen, P. R. 2001. Analysis of terrestrial and martian volcanic compositions using thermal emission spectroscopy: 2. Application to martian surface spectra from the Mars Global Surveyor Thermal Emission Spectrometer. *Journal of Geophysical Research*, **106**, 14 733–14 746.

Hapke, B. 1993. *Theory of Reflectance and Emittance Spectroscopy*. Topics in Remote Sensing, **3**. Cambridge University Press, Cambridge.

Hapke, B. W. 2001. Space weathering from Mercury to the asteroid belt. *Journal of Geophysical Research*, **106**, 10 039–10 073.

Harloff, J. & Arnold, G. 2001. Near-infrared reflectance spectroscopy of bulk analogue materials for planetary crust. *Planetary Space Science*, **49**, 191–211.

Head, J. W., Murchie, S. L. *et al.* 2009. Volcanism on Mercury: evidence from the first MESSENGER flyby for extrusive and explosive activity and the volcanic origin of plains. *Earth and Planetary Science Letters*, **285**, 227–242.

Head, J. W., Chapman, C. R. *et al.* 2011. Flood volcanism in the northern high latitudes of Mercury revealed by MESSENGER. *Science*, **333**, 1853–1856, http://dx.doi.org/10.1126/science.1211997

Heater, D. J., Dunkin, S. K. & Wilson, L. 2003. Volcanism on the Marious Hills plateau: Observational analyses using Clementine multispectral data. *Journal of Geophysical Research*, **108**, 5017, http://dx.doi.org/10.1029/2002JE001938

Hiesinger, H. & Head, J. W., III 2006. New views of lunar geoscience: an introduction and overview. *In*: Ross, J. J. (ed.) *New Views of the Moon. Reviews in Mineralogy and Geochemistry*, **60**, 1–81.

Hiroi, T. & Pieters, C. M. 1994. Estimation of grain size and mixing ratios of fine powder misture of common

geologic minerals. *Journal of Geophysical Research*, **99**, 10 867–10 879.

Hiroi, T. & Sasaki, S. 2001. Importance of space weathering simulation products in compositional modeling of asteroids: 349 Dembowska and 446 Aeternitas as examples. *Meteoritics & Planetary Science*, **36**, 1587–1596.

Hunt, G. R., Salisbury, J. W. & Lenhoff, C. J. 1973*a*. Visible and near infrared spectra of minerals and rocks: VII. Acid igneous rocks. *Modern Geology*, **4**, 217–224.

Hunt, G. R., Salisbury, J. W. & Lenhoff, C. J. 1973*b*. Visible and near infrared spectra of minerals and rocks: VIII. Intermediate igneous rocks. *Modern Geology*, **4**, 237–244.

Hunt, G. R., Salisbury, J. W. & Lenhoff, C. J. 1974. Visible and near infrared spectra of minerals and rocks: IX. Basic and Ultrabasic igneous rocks. *Modern Geology*, **5**, 15–22.

Kaur, P., Bhattacharya, S., Chauhan, P., Ajai, & Kiran Kumar, A. S. 2013. Mineralogy of Mare Serenitatis on the near side of the Moon based on Chandrayaan-1 Moon mineralogy mapper (M3) observations. *Icarus*, **222**, 137–148.

Keszthelyi, L. P. 1995. A preliminary thermal budget for lava tubes on the Earth and planets. *Journal of Geophysical Research*, **100**, 20 411–20 420.

Keszthelyi, L., McEwen, A. S. & Thordarson, T. 2000. Terrestrial analogs and thermal models for Martian flood lavas. *Journal of Geophysical Research*, **105**, 15 027–15 050.

Klima, R. L., Pieters, C. M. & Dyar, M. D. 2007. Spectroscopy of synthetic Mg-Fe pyroxenes I: spinallowed and spin-forbidden crystal field bands in the visible and near-infrared. *Meteoritics & Planetary Science*, **42**, 235–253.

Klima, R. L., Pieters, C. M. & Dyar, M. D. 2008. Characterization of the 1.2 μm M1 pyroxene band: extracting cooling history from near-IR spectra of pyroxenes and pyroxene-dominated rocks. *Meteoritics & Planetary Science*, **43**, 1591–1604.

Klima, R. L., Dyar, M. D. & Pieters, C. M. 2011. Near-infrared spectra of clinopyroxenes: effects of calcium content and crystal structure. *Meteoritics & Planetary Science*, **46**, 379–395.

Klima, R. L., Izenberg, N. R. *et al.* 2013. Training the Ferrous Iron Content of Silicate Minerals in Mercury's Crust. Abstract 1602, presented at the 44th Conference on Lunar Planetary Science, Woodlands, Texas, March 18–22, 2013.

Lawrence, D. J., Hawke, B. R., Hagerty, J. J., Elphic, R. C., Feldman, W. C., Prettymann, T. H. & Vaniman, D. T. 2005. Evidence for a high-Th, evolved lithology on the Moon at Hansteen Alpha. *Geophysical Research Letters*, **32**, http://dx.doi.org/10.1029/2004GL022022

Lawrence, D. J., Feldman, W. C. *et al.* 2010. Identification and measurement of neutron-absorbing elements on Mercury's surface. *Icarus*, **209**, 195–209.

Le Maitre, R. W., Streckeisen, A. *et al.* (eds). 2002. *Igneous Rocks—A Classification and Glossary of Terms*. Cambridge University Press, Cambridge.

Lucey, P., Korotev, R. L. *et al.* 2006. Understanding the lunar surface and space–moon interactions. *In*: Ross, J. J. (ed.) *New Views of the Moon. Reviews in Mineralogy and Geochemistry*, **60**, 83–219.

Lucey, P. G. & Riner, M. A. 2011. The optical effects of small iron particles that darken but do not redden: evidence of intense space weathering on Mercury. *Icarus*, **212**, 451–462.

McSween, H. Y., Jr. & Treiman, A. H. 1998. Martian meteorites. *In*: Papike, J. J. (ed.) *Planetary Materials*. Reviews in Mineralogy, **36**. Mineralogical Society of America, Washington, DC, 6-1–6-53.

McSween, H. Y., Jr., Murchie, S. L. *et al.* 1999. Chemical, multispectral, and textural constraints on the composition and origin of rocks at the Mars Pathfinder landing site. *Journal of Geophysical Research*, **104**, 8679–8715.

McSween, H. Y., Arvidson, R. E. *et al.* 2004. Basaltic Rocks analyzed by the Spirit Rover in Gusev Crater. *Science*, **305**, 842–845, http://dx.doi.org/10.1126/science.3050842

McSween, H. Y., Ruff, S. W. *et al.* 2006*a*. Alkaline volcanic rocks from the Columbia Hills, Gusev Crater, Mars. *Journal of Geophysical Research*, **111**, E09S91, http://dx.doi.org/10.1029/2006JE002698

McSween, H. Y., Wyatt, M. B. *et al.* 2006*b*. Characterization and petrologic interpretation of olivine-rich basalts at Gusev Crater, Mars. *Journal of Geophysical Research*, **111**, E02S10, http://dx.doi.org/10.1029/2005JE002477

McSween, H. Y., Taylor, G. J. & Wyatt, M. B. 2009. Elemental composition of the Martian crust. *Science*, **324**, 736–739.

Middlemost, E. A. K. 1997. *Magmas, Rocks and Planetary Development: A Survey of Magma/Igneous Rock Systems*. Longman, Harlow.

Minitti, M. E., Mustard, J. F. & Rutherford, M. J. 2002. Effects of glass content and oxidation on the spectra of SNC-like basalts: applications to Mars remote sensing. *Journal of Geophysical Research*, **107**, 6-1–6-14, http://dx.doi.org/10.1029/2001JE00 1518

Mittlefehldt, D. W., McCoy, T. J., Goodrich, C. & Kracher, A.. 1998. Non-chondritic meteorites from asteroidal bodies. *In*: Papike, J. J. (eds) *Planetary Materials*. Reviews in Mineralogy, **36**. Mineralogical Society of America, Washington, DC, 4-1–4-195.

Moroz, L. V. & Arnold, G. 1999. Influence of neutral components on relative band contrasts in reflectance spectra of intimate mixtures: implications for remote sensing 1. Nonlinear mixing modeling. *Journal of Geophysical Research*, **104**, 14 109–14 122.

Moroz, L. V., Fisenko, A. V., Semionova, L. F., Pieters, C. M. & Korotaeva, N. N. 1996. Optical effects of regolith processes on S-Asteroids as simulated by Laser Shots on ordinary chondrite and other mafic materials. *Icarus*, **122**, 366–382.

Moroz, L., Schade, U. & Wasch, R. 2000. Reflectance Spectra of olivine-orthopyroxene-bearing assembleages at decreased temperatures: implications for remote sensing of asteroids. *Icarus*, **147**, 79–93, http://dx.doi.org/10.1006/icar.2000.6430

Neal, C. R. & Taylor, L. A. 1992. Petrogenesis of mare nasalts—A record of lunar volcanism. *Geochimica et Cosmochimica Acta*, **56**, 2177–2211.

Nicholis, M. G. & Rutherford, M. J. 2005. Pressure Dependence of Graphite–C–O Phase Equilibria and

its Role in Lunar Volcanism. Abstract 1732, presented at the 36th Conference on Lunar Planetary Science, League City, Texas, March 14–18, 2005.

Nittler, L. R., Starr, R. D. *et al.* 2011. The major-element composition of Mercury's surface from MESSENGER X-ray spectrometry. *Science*, **333**, 1847–1850.

Peitersen, M. N. & Crown, D. A. 1999. Down flow width behaviour of Martian and terrestrial lava flows. *Journal of Geophysical Research*, **104**, 8473–8488.

Pieters, C. M., Fischer, E. M., Rode, O. D. & Basu, A. 1993. Optical effects of space weathering on lunar soils and the role of the finest fraction. *Journal of Geophysical Research*, **98**, 20 817–20 824.

Pieters, C. M., Taylor, L. A. *et al.* 2000. Space weathering on airless bodies: resolving a mystery with lunar samples. *Meteoritics & Planetary Science*, **35**, 1101–1107.

Pilorget, C., Bibring, J.-P. THE MICROMEGA TEAM 2012. The MicrOmega Instrument Onboard ExoMars and Future Missions: An IR Hyperspectral Microscope to Analyze Samples at the Grain Scale and Characterize Early Mars Processes. Abstract 7006, presented at the Third International Conference on Early Mars: Geologic and Hydrologic Evolution, Physical and Chemical Environments, and the Implications for Life, Lake Tahoe, Nevada, May 21–25, 2012.

Pompilio, L., Sgavetti, M. & Pedrazzi, G. 2007. Visible and near-infrared reflectance spectroscopy of pyroxene-bearing rocks: new constraints for understanding planetary surface compositions. *Journal of Geophysical Research*, **112**, E01004, http://dx.doi.org/10.1029/2006JE002737

Poulet, F., Gomez, C. *et al.* 2007. Martian surface mineralogy from Observatoire pour la Mineralogie, l'Eau, les Glaces et l'Activite on board the Mars Express spacecraft (OMEGA/MEx): global mineral maps. *Journal of Geophysical Research*, **112**, E08S02, http://dx.doi.org/10.1029/2006JE002840

Poulet, F., Mangold, N. *et al.* 2009. Quantitative compositional analysis of Martian mafic regions using the MEx/OMEGA reflectance data: 2. Petrological implications. *Icarus*, **210**, 84–101.

Reider, R., Economou, T. *et al.* 1997. The chemical composition of Martian soil and rocks returned by the mobile alpha proton X-ray spectrometer: preliminary results in X-ray mode. *Science*, **278**, 1771–1774.

Riner, M. A., Lucey, P. G., McCubbin, F. M. & Taylor, G. J. 2011. Constraints on Mercury's surface composition from MESSENGER neutron spectrometer data. *Earth and Planetary Science Letters*, **308**, 107–114, http://dx.doi.org/10.1016/j.epsl.2011.05.042

Ruff, S. W. & Christensen, P. R. 2002. Bright and dark regions on Mars: particle size and mineralogical characteristics based on thermal emission spectrometer data. *Journal of Geophysical Research*, **107**, 5127, http://dx.doi.org/10.1029/2001JE001580

Russell, C. T. & Raymond, C. A. 2011. The Dawn Mission to Vesta and Ceres. *Space Science Review*, **163**, 3–23, http://dx.doi.org/10.1007/s11214– 011-9836-2

Sakimoto, S. E. H. & Zuber, M. T. 1998. Flow and convection cooling in lava tubes. *Journal of Geophysical Research*, **103**, 27 465–27 487.

Sakimoto, S. E. H., Crisp, J. & Baloga, S. M. 1997. Eruption constraints on tube-fed planetary lava flows. *Journal of Geophysical Research*, **102**, 6597–6613.

Sasaki, S., Nakamura, K., Hamabe, Y., Kurahashi, E. & Hiroi, T. 2001. Production of iron nanoparticles by laser irradiation in a simulation of lunar-like space weathering. *Nature*, **410**, 555–557.

Schaber, G. G., Boyce, J. M. & Moore, H. J. 1976. The scarcity of mapable flow lobes on the lunar maria: unique morphology of the imbrium flows. *In*: *Proceedings of the 7th Lunar Science Conference, Houston, Texas, March 15–19, 1976, Volume 3*. Pergamon Press, New York, 2783–2800.

Schade, U., Wäsch, R. & Moroz, L. 2004. Near-infrared reflectance spectroscopy of Ca-rich clinopyroxenes and prospects for remote spectral characterization of planetary surfaces. *Icarus*, **168**, 80–92.

Serventi, G., Carli, C. & Sgavetti, M. 2013*a*. Plagioclase Influence in Mixtures with Very Low Mafic Mineral Content. Abstract 1490, presented at the 44th Conference on Lunar Planetary Science, Woodlands, Texas, March 18–22, 2013.

Serventi, G., Carli, C., Sgavetti, M., Ciarniello, M., Capaccioni, F. & Pedrazzi, G. 2013*b*. Spectral variability of plagioclase-mafic mixtures 1): effects of chemistry and modal abundance in reflectance spectra of rocks and mineral mixtures. *Icarus*, **226**, 282–298, http://dx.doi.org/10.1016/j.icarus.2013.05.041

Sgavetti, M., Tramutoli, V., Pompilio, L. & Longhi, I. 2003. Field spectroscopy on Mount Etna. *In*: Blanco, A., Dotto, E. & Orofino, V. (eds) *Planetary Science, Proceedings of the Fifth Italian Meeting*, Gallipoli (Lecce), Italy, September 15–19, 2003. Alenia Spazio, Rome, 246–252.

Sgavetti, M., Pompilio, L. & Meli, S. 2006. Reflectance spectroscopy (0.3–2.5 um) at various scales for bulk-rock identification. *Geosphere*, **2**, 142–160.

Shearer, C. K., Hess, P. C. *et al.* 2006. Thermal and magmatic evolution of the Moon. *In*: Ross, J. J. (ed.) *New Views of the Moon Reviews in Mineralogy and Geochemistry*, 365–518.

Sleep, N. H. 2000. Evolution of the mode of convection within terrestrial planets. *Journal of Geophysical Research*, **105**, 17 563–17 578, http://dx.doi.org/10.1029/2000JE001240

Solomon, S. C., McNutt, R. L., Jr. *et al.* 2008. Return to Mercury: a global perspective on MESSENGER's first Mercury flyby. *Science*, **321**, 59–62.

Spudis, P. D., McGovern, P. J. & Kiefer, W. S. 2013. Large shield volcanoes on the Moon. *Journal of Geophysical Research*, **118**, 1063–1081, http://dx.doi.org/10.1002/jgre.20059

Strazzulla, G., Dotto, E., Binzel, R., Brunetto, R., Barucci, M. A., Blanco, A. & Orofino, V. 2005. Spectral alteration of the Meteorite Epinal (H5) induced by heavy ion irradiation: a simulation of space weathering effects on near-Earth asteroids. *Icarus*, **174**, 31–35.

Streckeisen, A. 1978. IUGS Subcommission on the Systematics of Igneous Rocks. Classification and nomenclature of volcanic rocks. Recommendations and suggestions. *Neues Jahrbuch fur Mineralogy*, **143**, 1–14.

Sunshine, J. M. & Pieters, C. M. 1991. Identification of modal abundances in the spectra of natural and laboratory pyroxene mixtures: a key component for remote analysis of lunar basalts. *Abstracts of the Lunar and Planetary Science Conference*, **22**, 1361–1362.

Sunshine, J. M. & Pieters, C. M. 1993. Estimating modal abundances from the spectra of natural and laboratory pyroxene mixtures using the modified Gaussian model. *Journal of Geophysical Research*, **98**, 9075–9087.

Sunshine, J. M. & Pieters, C. M. 1998. Determining the composition of olivine from reflectance spectroscopy. *Journal of Geophysical Research*, **103**, 13 675–13 688.

Sunshine, J. M., Pieters, C. M. & Pratt, S. F. 1990. Deconvolution of mineral absorption bands: an improved approach. *Journal of Geophysical Research*, **95**, 6955–6966.

Taylor, G. J., Warren, P., Ryder, G., Delano, J., Pieters, C. & Lofgren, G. 1991. Lunar rocks. *In*: Heiken, G., Vaniman, D. & French, B. (eds) *The Lunar Source Book: A User's Guide to the Moon*. Cambridge University Press, Cambridge, 183–284.

Tompkins, S. & Pieters, C. M. 2010. Spectral characteristics of lunar impact melts and inferred mineralogy. *Meteoritics & Planetary Science*, **45**, 1152–1169.

Waenke, H., Bruckner, J., Dreibus, G., Rieder, R. & Ryabchikoy, I. 2001. Chemical composition of rocks and soils at the pathfinder site. *Space Science Review*, **96**, 317–330.

Warren, P. H. & Wasson, J. T. 1979. The origin of KREPP. *Reviews of Geophysics and Space Physics*, **17**, 73–88.

Watters, T. R., Murchie, S. L., Robinson, M. S., Solomon, S. C., Denevi, B. W., André, S. L. & Head, J. W. 2009. Emplacement and tectonic deformation of smooth plains in the Caloris basin, Mercury. *In*: Solomon, S. C., Prockter, L. M. & Blewett, D. T. (eds) *MESSENGER's First Flyby of Mercury*. *Earth and Planetary Science Letters*, **285**, 309–319.

Weider, S. Z., Nittler, L. R. *et al.* 2012. Chemical heterogenity on Mercury's surface revealed by the MESSENGER X-ray spectrometer. *Journal of Geophysical Research*, **117**, E00L05, http://dx.doi.org/10.1029/2012JE004153

Weider, S. Z., Nittler, L. R., Starr, R. D. & Solomon, S. C. 2013. Distribution of Iron on the Surface of Mercury from MESSENGER x-ray Spectrometer Measurements. Abstract 2189, presented at the 44th Conference on Lunar Planetary Science, Woodlands, Texas, March 18–22, 2013.

Yamada, M., Sasaki, S. *et al.* 1999. Simulation of space weathering of planet-forming materials: nanosecond pulse laser irradiation and proton implantation on olivine and pyroxene samples. *Earth Planets Space*, **51**, 1255–1265.

Yon, S. A. & Pieters, C. M. 1988. Interactions of light with rough dielectric surfaces: spectral reflectance and polarimetric properties. *In*: Ryder, G. (ed.) *Proceedings of the 19th Lunar Science Conference*. Cambridge University Press, New York, 581–592.